

# On the Interference As Noise Approximation in OFDMA/LTE Networks

Donald Parruca\* and James Gross†

\*UMIC Research Centre, RWTH Aachen University, Germany

†School of Electrical Engineering, KTH Royal Institute of Technology, Sweden  
parruca@umic.rwth-aachen.de

**Abstract**—In this paper we generalize analytical performance models for proportional fair scheduling in OFDMA/LTE networks. We address the issue of modelling multiple fading interferers present in practical deployments. Specifically, we elaborate on the stochastic modelling of SINR-distribution for which we derive the rate expectation of instantaneously scheduled resources. The resulting analytical performance model is validated by means of simulations considering realistic network deployments. Compared with related work, our model demonstrates a significantly higher accuracy for long-term rate estimation. We illustrate the utility of such high-precision models by studying the impact on terminal assignment in fractional frequency reuse. Simply by using a suitable estimation model, cell-edge throughput can be improved up to 50%.<sup>1</sup>

## I. INTRODUCTION

Cellular network operators are constantly facing an increasing demand for higher mobile data rates. To cope with it, several approaches are proposed for upcoming evolution of mobile networks. Among others, advanced antenna techniques, frequency reuse of one and cell densification in regions with high capacity requirement are important system features to be exploited. In the last approach the system capacity is increased by deploying base stations (cells) closely to each other (a few tens to a couple of hundred meters). However, such approaches should be handled with care as co-channel interference caused from full frequency reuse of the radio spectrum severely impacts communication capacity. Careful planning as well as dynamic inter-cell interference coordination techniques are needed for an efficient network operation.

This efficient operation of the network requires essentially dynamic long-term system decisions at run-time with respect to the performance of the system. Long-term refers here to timespans in the range of seconds and applies mainly to admission control, load balancing, cell association as well as intercell interference coordination. This is contrasted by the short duration of the transmit slots of LTE systems in the range of milliseconds and the fast scheduling occurring once per slot. Any such long-term decision requires a precise modelling of link capacity over this time span. However, this modelling is involved for LTE systems due to several aspects. On the one hand, link capacity over longer time spans depends on

random variables such as the channel gain of the signal-of-interest as well as the interfering signals. As LTE is designed to cope with a frequency reuse of one, many potential interfering sources can interact with the signal of interest. Furthermore, instantaneous link qualities translate into data rates depending on the link adaptation technique in LTE. Most importantly, uniform modulation and coding over several resource blocks makes the translation of a statistical link quality model into a corresponding link rate model difficult. Thirdly, LTE features dynamic (fast) resource allocation per slot (i.e. on a millisecond base) which provides a performance boost but leads also to an impact on the statistical link model. Summarizing, precise link quality models are hard to determine for LTE networks.

In related work, this has lead to the usage of several simplifications to steer long-term dynamic operations of the network. For instance, in [1] and [2], this has lead to the simplification of the instantaneous signal-to-interference-and-noise ratio (SINR) as exponentially distributed to steer long-term dynamic operations of the network. This model is also referred to as *interference-as-noise* model, because the impact due to interference is averaged and modelled as an additional constant noise component in the SINR expression. Meanwhile, in [3] the SINR distribution is assumed as Gaussian distributed. Simulations and analytical evaluations from [4] showed that both these simplifications are very similar in rate prediction performance. On the other side, the SINR distribution is not exponential and a precise modelling of the SINR together with the consideration of the dynamic resource allocation has a significant divergence from the approximate model [4]. Nevertheless, the work presented there did not consider multiple interfering sources which are in general present in practical LTE network deployments.

In this paper we generalize our previous work in [4] and address the issue of multiple interferers and uniform modulation and coding. Precisely, for an exact stochastic model of the SINR-distribution for many interferers, we model analytically the impact due to dynamic (fast) resource scheduling (i.e. proportional fair scheduling) and uniform modulation and coding in the down-link of LTE systems. This model is evaluated based on simulations by considering realistic channel and deployment data. We show that with respect to related work, we provide the most accurate model for long-term rate estimates in LTE systems under the mentioned conditions. While the performance difference is large at the cell edge,

<sup>1</sup>This work was partially supported by the DFG Cluster of Excellence on Ultra High-Speed Mobile Information and Communication (UMIC), German Research Foundation grant DFG EXC 89.

it becomes smaller at the cell centre. A further aspect in the model precision is the number of interfering sources. Finally, for standard fractional frequency reuse (FFR) we demonstrate the impact from the high-precision rate model, which gives significant performance improvements in FFR systems simply from a more accurate rate estimation. This strengthens our claim that exact performance models are required for efficient operation of upcoming LTE networks.

## II. SYSTEM MODEL

We consider the downlink communication of an OFDMA/LTE multi-cellular network deployment. The frequency spectrum is split into  $N$  chunks of subsequent  $N_S$  sub-carriers also known as resource blocks (RB), used for the transmission of  $N_C$  OFDM symbols. Time is slotted into so called transmission time intervals (TTI) of duration  $T_{TTI}$ . Every time slot the base station, being the central coordination point of transmissions, dynamically allocates resources to mobile terminals. Among the vast choice of resource allocation algorithms, proportional fair scheduling (PFS) has found a very wide acceptance, due to its ability to take advantage of multi-user diversity and provide fairness in resource allocation [4],[5]. We assume in this paper that the base station is performing resource allocation according to PFS.

Assuming  $I$  interfering base stations are causing co-channel interference instantaneously transmitting in the same frequency band, the total instantaneous random interference power is given by as  $Y(t) = \sum_{i=1}^I Y_i(t)$ . Considering constant noise power level of  $N_0$  the signal-to-interference-noise ratio (SINR) realization at terminal  $j$  on RB  $n$  is thus represented by:

$$(1) \quad \gamma_{j,n}(t) = \frac{X_{j,n}(t)}{\sum_{i=1}^I Y_{j,n}^i(t) + N_0}.$$

Mobile terminals periodically send channel quality information feedback to the serving base station. It is a measure directly depending on the SINR  $\gamma_{j,n}(t)$  telling the highest modulation and coding scheme (MCS) that the reporting mobile terminal can decode so that a target bit error rate is maintained. The spectral efficiency of the MCS used is given by  $C(\gamma_{j,n}(t))$ . We consider the mapping used in [6]. At the base station (BS) side two metrics can be used for scheduling, it can be either the potential instantaneous rate that RBs can transport:  $\frac{N_S N_C}{T_{TTI}} C(\gamma_{j,n}(t))$  or the RB's SINR value obtained from the inverse spectral efficiency function  $C^{-1}(\gamma_{j,n}(t))$ . In this paper we work with with an SINR-based proportional fair scheduling scheduler. For each MS and RB, the proportional fair scheduling algorithm based on the previous feedbacks builds the average SINR  $\bar{\gamma}_{j,n}$  during the last  $W$  TTIs:

$$(2) \quad \bar{\gamma}_{j,n}(t) = \frac{1}{W} \sum_{i=t-W}^{t-1} \gamma_{j,n}(i).$$

Then, the scaled SINR  $\hat{\gamma}_{j,n} = \frac{\gamma_{j,n}}{\bar{\gamma}_{j,n}}$  is used as a priority metric in allocating the resources. The scheduling decision  $M_{j,n} = 1$

on assigning resource block  $n$  to MS  $j$  is taken if this terminal has the highest scaled SINR on the RB under consideration:

$$(3) \quad \forall n : j_n^*(t) = \arg \max_{j \in \mathcal{J}} \hat{\gamma}_{j,n}(t).$$

In case at time instant  $t$  a non-empty subset of RBs  $A_j \subseteq \{1, \dots, N\}$  have been scheduled to mobile station  $j$ , then a common modulation and coding scheme  $m_j$  is used for transport block transmission. There are several ways how a MCS might be chosen, in this work we assume the application of a conservative approach, i.e. for a robust transmission the common MCS is set according to the lowest reported CQI of the scheduled subset:

$$(4) \quad m_j = \min_{n \in A_j} m_j^n.$$

## III. THROUGHPUT EXPECTATION IN OFDMA NETWORKS

For the throughput expectation under proportional fair scheduling, the basic probability density and cumulative distribution functions without the impact of the scheduler need first to be computed. In interference limited scenarios  $Y(t) \gg N_0$  the signal-to-interference (SIR) ratio distribution function is sufficient. However, for comparable power levels of interference and noise, corresponding functions of SINR are more preferable. The probability density function (PDF) and cumulative distribution functions (CDF) were already addressed in [7]. The SIR CDF is built according to an infinite sum of elements of a series. Additionally, the SIR distribution functions are defined for only two extreme cases: interferers have the same mean interference power or mutually different. Scenarios where groups of interferers have same mean but mutually different between groups is not defined. For the sake of completeness we derive in the following the SINR PDF and CDF for any possible configuration of interfering sources. The corresponding SINR CDF is built based on a limited number of series elements which allows numerical evaluation through software.

1) *Basic SINR PDF*: We consider here a Rayleigh-Rayleigh fading model. Both the power distribution of signal-of-interest  $f_X(x)$  and of single interfering sources  $f_{Y_i}(y)$  are exponentially distributed like:

$$(5) \quad f_X(x) = \lambda_0 \exp(-\lambda_0 x), \quad x \geq 0,$$

$$(6) \quad f_{Y_i}(x) = \lambda_i \exp(-\lambda_i y), \quad x \geq 0.$$

where  $X$  and  $Y$  are respectively the powers of the fading signal-of-interest and interference. Meanwhile,  $\lambda = \frac{1}{P \cdot \bar{h}}$  is the parameter of the exponential distribution, equal to the inverse of the average received power. For a constant transmit power  $P$  and path-loss  $\bar{h}$ , the parameter is given by  $\lambda = \frac{1}{P \cdot \bar{h}}$ . In the following we will denote by  $\lambda_0$  the parameter of the signal-of-interest and by  $\lambda_1, \dots, \lambda_I$  the corresponding parameters of the individual interfering sources. Given the above definitions we are interested in the cumulative distribution function (CDF)  $F_Z(z)$  and probability density function (PDF)  $f_Z(z)$  of the SINR.

The interfering sources can be arranged according to their parameter  $\lambda_i$  in tuples  $(r_t, \lambda_t)$ , where  $r_t$  denotes the number of

interfering sources having the same parameter  $\lambda_t$ . Denote the amount of tuples by  $p$ , then the total number of interferers can be expressed as  $I = \sum_{t=1}^p r_t$ . The sum of  $r_t$  i.i.d. exponential random variables each with parameter  $\lambda_t$  (from the tuple  $(r_t, \lambda_t)$ ) is well known to be gamma distributed:

$$(7) \quad f_{Y_t}(y) = \frac{\lambda_t e^{-\lambda_t y} (\lambda_t y)^{r_t-1}}{(r_t-1)!} \quad y > 0.$$

Then, the total interference power  $f_Y(y)$  can be considered as the sum of  $p$  gamma distributed random variables with corresponding parameters  $(r_t, \lambda_t)$ . In order to analytically deal with  $Y = \sum_{t=1}^p Y_t$  we utilize the generalized integer gamma distribution law, which was introduced by Coelho [8], describing the distribution of the sum of gamma distributed random variables with *integer* shape parameter  $r_t$  and unique rate parameters  $\lambda_j$ . It is constructed as a sum of finite elements and is quite easy to evaluate numerically by software. From Coelho's work [8] we have:

$$(8) \quad f_Y(y) = K \sum_{t=1}^p P_t(y) e^{-\lambda_t y}, \quad (y > 0)$$

and

$$(9) \quad F_Y(y) = 1 - K \sum_{t=1}^p P_t^*(y) e^{-\lambda_t y}, \quad (y > 0),$$

where

$$(10) \quad K = \prod_{t=1}^p \lambda_t^{r_t}, \quad P_t(y) = \sum_{k=1}^{r_t} c_{t,k} y^{k-1},$$

and

$$(11) \quad P_t^*(y) = \sum_{k=1}^{r_t} c_{t,k} (k-1)! \sum_{s=0}^{k-1} \frac{y^s}{s! \lambda_t^{k-s}},$$

with

$$(12) \quad c_{t,r_t} = \frac{1}{(r_t-1)!} \prod_{\substack{s \neq t \\ s=1}}^p (\lambda_s - \lambda_t)^{-r_s}, \quad t = 1, \dots, p,$$

and

$$(13) \quad c_{t,r_t-k} = \frac{1}{k} \sum_{s=1}^k \frac{(r_t - k + s - 1)!}{(r_t - k - 1)!} R(s, t, p) c_{t,r_t-(k-s)},$$

$$(t = 1, \dots, p; k = 1, \dots, r_t - 1)$$

where

$$(14) \quad R(s, t, p) = \sum_{\substack{k \neq t \\ k=1}}^p r_k (\lambda_t - \lambda_k)^{-s}, \quad (s = 1, \dots, r_t - 1).$$

Considering noise power to be constant, the PDF of the disturbing component (interference + noise) can be computed as a shift operation  $f_{Y+N_0}(y) = f_Y(y - N_0)$ . Following

standard rules of PDF transformation (found in [9]) we can obtain the cumulative distribution function of the SINR:

$$(15) \quad F_Z(z) = 1 - K \sum_{t=1}^p P_t^{**}(z) e^{-\lambda_0 N_0 z},$$

where

$$(16) \quad P_t^{**}(z) = \sum_{k=1}^{r_t} c_{t,k} (k-1)! \frac{1}{(\lambda_t + \lambda_0 z)^k}.$$

Deriving  $F_Z(z)$  with respect to variable  $z$  the corresponding density function can be obtained:

$$(17) \quad f_Z(z) = K \sum_{t=1}^p P_t^{***}(z) e^{-N_0 \lambda_0 z}$$

where

$$(18) \quad P_t^{***}(z) = \sum_{k=1}^{r_t} c_{t,k} (k-1)! \frac{\lambda_0 (k + N_0 (\lambda_t + \lambda_0 z))}{(\lambda_t + \lambda_0 z)^{k+1}}.$$

2) *Scheduled SINR PDF transformation:* It is well known that proportional fair scheduling beneficially transforms the probability density functions of the scheduled resource blocks. Nevertheless, the transformation is tightly coupled with the basic SINR PDF and CDF functions developed in the previous section. From [4] the scheduled SINR PDF transformation is given as:

$$(19) \quad f_{Z_{j,n}|M_{j,n}=1}(z) = \frac{\prod_{\forall i \neq j \in \mathcal{J}} F_{Z_{i,n}} \left( \frac{E[Z_{i,n}]}{E[Z_{j,n}]} \cdot z \right) \cdot f_{Z_{j,n}}(z)}{P(M_{j,n} = 1)},$$

where  $E[Z_{j,n}]$  is the expectation of the SINR modelling  $\bar{\gamma}_{j,n}$  for a sufficiently large window size  $W$ . The corresponding CDF can then be computed from the following integral:

$$(20) \quad F_{Z_{j,n}|M_{j,n}=1}(z) = \int_0^z f_{Z_{j,n}|M_{j,n}=1}(s) ds.$$

3) *Throughput expectation:* In LTE it is required that instantaneously scheduled resource blocks should be transmitted with a common modulation and coding scheme (MCS). This feature has implications on rate modelling as the MCS decision is based on the joint SINR realisations of the assigned RBs. A rate model for such a system is introduced in [4] expressing the total rate per MS as the sum over all possible RB assignments  $\mathcal{A}$ :

$$(21) \quad \mathcal{R}_j = \sum_{\forall \mathcal{A} \subseteq \{1, \dots, N\}} \mathcal{R}_{j,\mathcal{A}},$$

where  $\mathcal{A}$  is the non-empty subset of RBs:  $\mathcal{A} \subseteq \{1, \dots, N\}$ . We work here with a conservative MCS selection approach based on the worst SINR realisation of simultaneously assigned RBs, hence the rate expectation for the subset  $\mathcal{A}$  is based on the

minimum order statistic  $f_{Z_{j,A}^{\min}|M_{j,A}=1}(z)$  of the scheduled SINR PDF as follows:

$$(22) \quad \mathcal{R}_{j,A} = P_{j,A} |\mathcal{A}| \frac{R \cdot S}{T_{\text{TTI}}} \int_0^\infty f_{Z_{j,A}^{\min}|M_{j,A}=1}(z) \cdot C(z) dz,$$

where  $P_{j,A}$  is the probability scheduling subset  $\mathcal{A}$  to terminal  $j$  expressed as:

$$(23) \quad P_{j,A} = \prod_{n \in \mathcal{A}} P(M_{j,n} = 1) \prod_{n \notin \mathcal{A}} [1 - P(M_{j,n} = 1)],$$

which is composed from the scheduling probability of a single RB computed as follows:

$$(24) \quad P(M_{j,n} = 1) = \int_0^\infty f_{\hat{Z}_{j,n}}(z) \cdot \prod_{\forall i \neq j \in \mathcal{J}} F_{Z_{i,n}}(E[Z_{i,n}] \cdot z) dz.$$

The minimum order statistic of the scheduled SINR is represented as follows:

$$(25) \quad f_{Z_{j,A}^{\min}|M_{j,A}=1}(z) = \sum_{n \in \mathcal{A}} \left[ f_{Z_{j,n}|M_{j,n}=1}(z) \cdot \prod_{\forall m \neq n \in \mathcal{A}} (1 - F_{Z_{j,m}|M_{j,m}=1}(z)) \right].$$

Although a high degree of detail was included in the rate estimation model, still some deviation is to be expected due to lack of modelling of correlation in time and frequency, and different distributions in fading (i.e. no Rayleigh distribution).

#### IV. NUMERICAL ANALYSIS

In this section, we evaluate our model in two sets. Initially, we validate both the basic and scheduled SINR distributions. In a second step, we then compare the rate estimates of our model with the interference as noise estimate and benchmark it with values from an LTE simulator. We choose the urban area of the city of Munich as a simulation playground. In order to employ accurate path loss values a ray prediction algorithm introduced in [10] is used. A 3D model of the city together with the position of a base station and antenna pattern serve as input in predicting the radio signal strength in the surrounding area of the base stations. Knowing the position of MSs in the map, we can easily relate to the predicted path loss values from the propagation map. They are further used into our LTE system level simulator.

We consider in our evaluation an LTE-like network deployment operating with a bandwidth of 5 MHz, equal to 25 transport resource blocks used for the transmission of 14 symbols and always aggregating 12 subcarriers to one resource block. The center frequency is equal to 1.8 GHz and 20 W transmission power per sector is assumed. Transmission is time-slotted with duration of  $T_{\text{TTI}} = 1\text{ms}$ . Fast fading was generated according to the Jake's model with a Doppler shift of 70 Hz and delay spread of 991 ns being parameters according to the Extended Typical Urban Model [11]. The simulated links are SISO communication channels using  $120^\circ$

sectorized antennas with 15 dBi maximal gain for the eNB and omnidirectional antenna for MS. From the overall network deployment we select an arbitrary cell and simulate the downlink communication for different drops of mobile stations. The communication is limited by co-channel interference generated from the surrounding cells, all operating in the same frequency band. A view of the cell footprint, which is also the region with the strongest long-term SINR is represented in Figure 1.

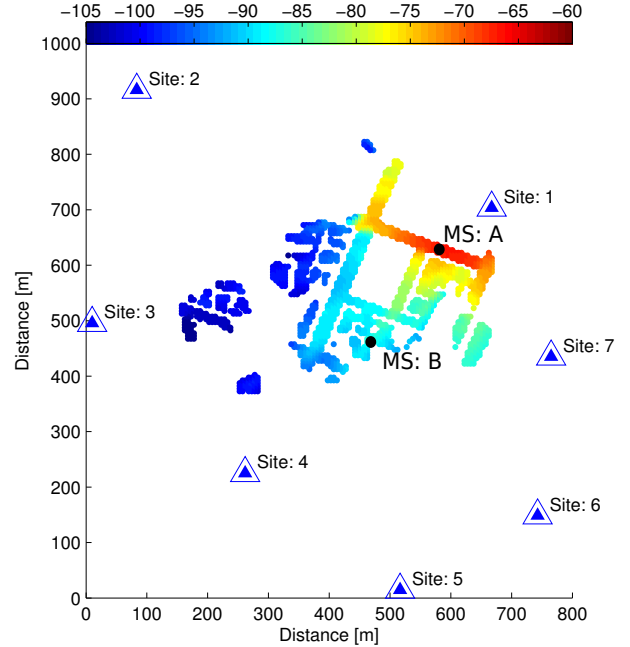


Fig. 1: Cell footprint and pathloss from Site 1.

##### A. SINR Model Validation

For the SINR model validation we simulate the downlink communication of a random drop of 20 terminals under the effect of three interfering sources (Site 3, 4 and 7). The cumulative distribution function of SINR developed in the previous section is validated here for two extreme locations that might arise in a cell: cell core (MS A in Fig. 1) and cell edge (MS B in Fig. 1). The SINR of a fixed resource block assuming flat fading for the corresponding subcarriers was simulated. The instantaneous SINR realizations at the probe locations were periodically sampled every 1 millisecond for a total simulation time of six seconds. We will refer to the statistics of this measurement as the simulated basic SINR. Additionally, we sampled also the scheduled SINR realization to one of the shown terminals. Based on these data, we do the validation of the theoretical models of SINR distributions. We compare the theoretical models of basic and scheduled SINR distributions (respectively Formulas (15) and (20)) with the simulated CDF curves. The results are plotted in Figure 2.

We can observe that the CDF curves of the basic SINR observations and the theoretical model are in general matching which indicates the validity of our analytical model. A good match can be also observed for the scheduled SINR

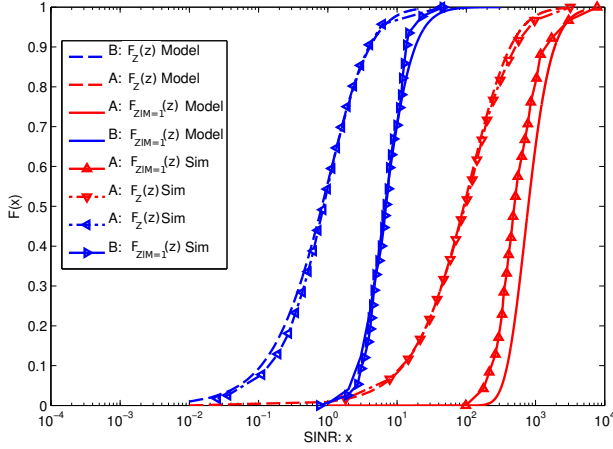


Fig. 2: Model validation of the basic  $F_Z(z)$  and scheduled  $F_{Z|M_{j,n}=1}$  SINR distributions at MS locations A and B.

distribution, especially for the low SINR regime. For high-SINR regimes the theoretical model overestimates scheduled SINR. This basically has two different reasons. Firstly, the approximation of the window size  $W$  which in our simulations was limited (1000 TTIs) long, is not time-limited in the theoretical model, as we take the expectation over the random variable. Secondly, the correlation in time and frequency are also not modelled in the theoretical model. Nevertheless, as shown in the next section this bias has only a weak impact on the precision of the rate estimation for the corresponding terminals.

### B. Rate Model Validation in Practical Deployments

For the rate model validation the prediction accuracy for each drop of mobile stations was measured. We simulated 30 scenarios (mobile terminal drops) of 20 mobile terminals uniformly distributed throughout the cell under investigation. Each drop was further simulated 10 times for different seeds of random number generators, their mean will be referred as *observed rates*  $\hat{\mathcal{R}}_j$ . For each UE drop, we compute the corresponding theoretical rate from Formula (26). From these data we compute the relative error  $\epsilon_j$  of rate predictions like  $\epsilon_j = |\hat{\mathcal{R}}_j - \mathcal{R}_j| \cdot 100 / \hat{\mathcal{R}}_j$ .

The accuracy analysis was further performed also for an alternative, simplified model widely used in the literature [1], [2]. Firstly, the impact of common modulation and coding schemes is ignored. This relaxes the dependency due to common MCS between different resource blocks in the rate model, leading to the following expression  $\hat{\mathcal{R}}_j = \sum_{n=1}^N \mathcal{R}_{j,n}$ , where  $\mathcal{R}_{j,n}$  is the rate expectation per RB computed like following:

$$\mathcal{R}_{j,n} = \frac{N_S \cdot N_C}{T_{TTI}} \int_0^\infty C(z) \prod_{\forall i \neq j} F_{\tilde{Z}_{i,n}} \left( \frac{E[\tilde{Z}_{i,n}]}{E[\tilde{Z}_{j,n}]} \cdot z \right) \cdot f_{\tilde{Z}_{j,n}}(z) dz. \quad (26)$$

Secondly, instead of accounting for the interference term in the SINR formula according to its precise distribution, the

average of the interference power is summed up and added to the noise as constant parameter. Therefore, the SINR becomes exponentially distributed. Hence, interference power is considered not being as a sum of exponentially distributed random variables, but as noise with constant power:  $P_{j,n}^i = \sum_i p_{j,n}^i \bar{h}_j^i$ . Such a model is widely used in [12], [13], [14] and [15]. We will name this rate model as ‘‘Interference as Noise’’ (IaN) whose instantaneous SINR distribution is assumed as:

$$F_{\tilde{Z}_{j,n}}(z) = 1 - \exp\left(-\frac{P_{j,n}^i + \eta}{P_{j,n}^s} \cdot z\right). \quad (27)$$

Still the effect of multi-user diversity gain is modelled by plugging the ‘‘Interference as Noise’’ PDF and CDF functions in Formula (26).

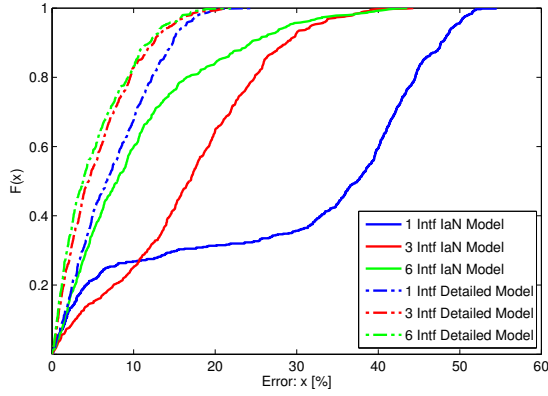
The error CDF curves for both models are shown in Figure 3a. There we show the influence that increasing number of interferers have on the prediction accuracy. As it can be noticed the exact model remains relatively unaffected by the increasing number of interferers. The worst prediction error (approx. 50%) appears for the case of a single interfering source and diminishes as the number of interferers increases. The increasing number of interferers reduces the deviation of the total received interfering power. This causes the total interference power to become more similar to an additive component to noise. The error distribution among the cell is represented in Figures 3b, 3c and 3d where we notice that also for typical practical scenarios of 3 interfering base stations per sector the rate prediction accuracy of IaN model remains still low for cell-edge terminals. Rate estimations for mobile stations being nearer to the interfering source have the highest discrepancy.

We believe that such differences of accuracy for different models have an important impact on long-term system decisions such as inter-cell interference coordination, handover decisions, admission control or load-balancing. Therefore, we study in the next section the impact that highly detailed models have on one of these approaches, namely inter-cell interference coordination.

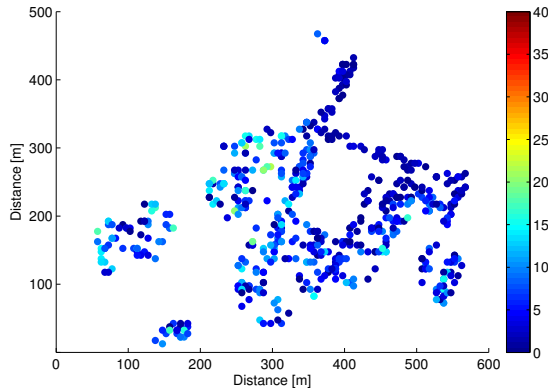
## V. ACCURACY IMPACT ON FRACTIONAL FREQUENCY REUSE SCHEMES

Fractional frequency reuse approaches [1],[16],[17] assign the available frequency spectrum in each cell exclusively to two main groups of users, namely cell center and cell-edge located users. An orthogonal spectrum for cell-edge terminals is allocated to the neighbouring cells, avoiding interference from first-tier base stations. On the other hand, centrally located terminals are less susceptible to inter-cell interference, than cell-edge ones. Hence the destined spectrum for such users is fully reused in all cells.

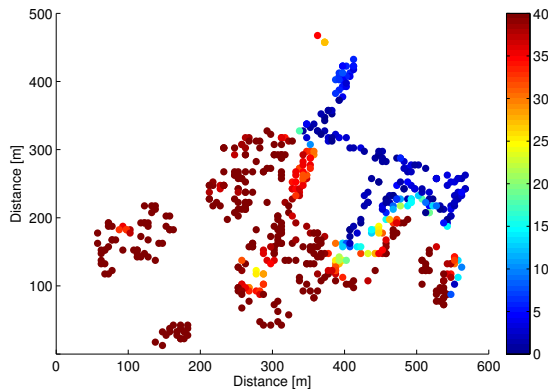
Many FFR schemes base their decision purely on the mobile terminal distance to the base station. For example in [16] threshold values for the categorisation of cell-edge and cell center are used. Such kind of categorisation is sub-optimal, because the communication link is subject not only to path-loss (proportional with the distance to the serving base station)



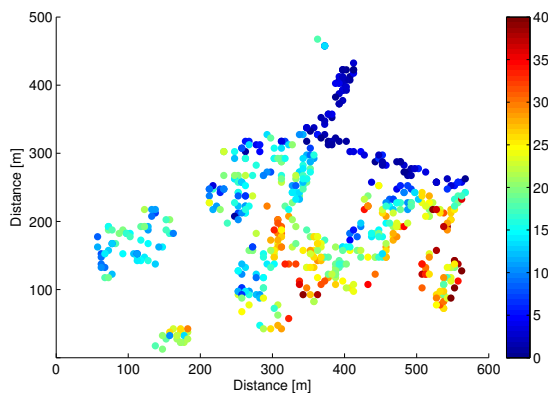
(a) Error CDF of IaN model



(b) Error in % of detailed model for 3 intfs. (Site 3,4,7)



(c) Error in % of IaN model for 1 intf. (Site 3)



(d) Error in % of IaN model for 3 intfs. (Site 3,4,7)

Fig. 3: Error of IaN for different number of interfering sources

but also to shadow fading (resulting from obstructing objects in the communication path). Therefore in [17] optimal threshold values of long term SINR for an optimum allocation are searched. Nevertheless, threshold based approaches are not conscious of the impact their decisions have on the resulting performance of mobile terminals.

Instead, in the following we elaborate on the user classification scheme of the strict-FFR approach used in [16] shown to perform better than soft frequency reuse ICIC schemes. In strict-FFR the cell-edge frequency spectrum is exclusively assigned to exterior users. On the other side, interior mobile stations do not share any spectrum with cell-edge ones. The cell-edge spectrum is reused with a factor of two in case of one interfering source and with a factor of three when more interfering cells are available. The classification algorithm used here is a max-min optimization problem. Initially all terminals are assumed to be centrally located and their potential rate is computed according to one of the rate models (Formula (21) or (IV-B)) introduced in this paper. Initially the terminal having the worst predicted rate is considered for reallocation into the cell-edge pool. If the predicted minimal rate of the cell is increased (based on the throughput expectation model used) the reallocation algorithm proceeds with the next worst rate predicted terminal from the cell center pool. The reallocation of cell center to cell edge users proceeds as long as the minimal rate of the system is increased. When a degradation of the minimum rate is noticed, the categorisation process terminates. As it can be noticed it is a simple but efficient categorisation algorithm where the rate prediction model plays a crucial role.

For the case of a single interferer, 3 RBs per cell were assigned for the cell edge users. Meanwhile, for a higher number of interferers 5 RBs were allocated to terminals belonging to the edge pool. We evaluated the quality of system allocations based on system level simulations and measured the throughput for each terminal. Based on these data we built the corresponding rate empirical CDF curves and show the results in Figure 4. We are applying a max-min optimization algorithm, which sacrifices the rate of terminals being in good channel conditions to improve the rate of bad ones. Therefore, the focus relies on the cell-edge located users and we will concentrate on the lower 50% percentile of the rate ECDF curves.

Figure 4 represents the rate empirical CDF curves for the system operating under the influence of 1-3 and 6 interference sources. Compared with frequency reuse of one, allocations based on the detailed rate model have always a positive impact on the cell-edge located terminals (see 5% percentile). The contrary is true for the interference as noise model when a single interfering source is present. Although the performance of cell-edge terminals based on the ‘‘IaN’’ allocation improves with the increasing number of interferers it still remains to some point inferior to allocations based the detailed rate model. For example, for a typical scenario of a sector surrounded from three other interfering ones a 30% performance improvement (from 300 kbps to 400 kbps) is obtained solely working on a more precise model. As the number of interferers

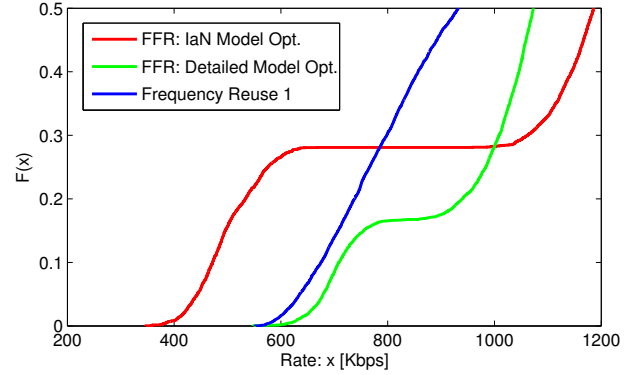
increases (scenarios of 6 interferers) the performance of both models is comparable.

## VI. CONCLUSIONS

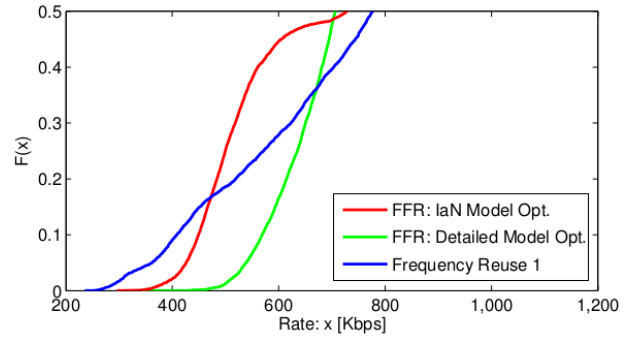
In this paper we introduced a highly detailed rate-prediction model of OFDMA/LTE systems operating with proportional fair scheduling at the base station. It precisely models system aspects like the effect of multiple fading interferers and modulation and coding scheme constraints, showing to have an important aspect on the rate prediction accuracy. Based on the the observed significant system improvements through inter-cell interference coordination we conclude that an increased level of detail in rate prediction models has a positive influence on long-term system decisions.

## REFERENCES

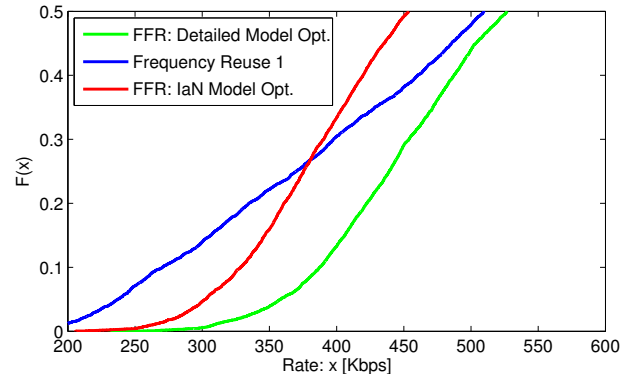
- [1] K. Son, S. Chong, and G. d. Veciana, "Dynamic association for load balancing and interference avoidance in multi-cell networks," *IEEE Transactions on Wireless Communications*, vol. 8, no. 7, pp. 3566–3576, 2009.
- [2] R. Combes, Z. Altman, M. Haddad, and E. Altman, "Self-optimizing strategies for interference coordination in OFDMA networks," in *Proceedings of IEEE International Conference on Communications Workshops (ICC)*, 2011, pp. 1–5.
- [3] E. Liu and K. Leung, "Expected throughput of the proportional fair scheduling over rayleigh fading channels," *IEEE Communications Letters*, vol. 14, no. 6, pp. 515–517, Jun 2010.
- [4] D. Parruca, M. Grysla, S. Goertzen, and J. Gross, "Analytical Model of Proportional Fair Scheduling in Interference-limited OFDMA/LTE Networks," in *Proc. of IEEE 78th Vehicular Technology Conference: VTC2013-Fall*, Sept. 2013.
- [5] S. Nonchev and M. Valkama, "A new fairness-oriented packet scheduling scheme with reduced channel feedback for OFDMA packet radio systems," *IJCNIS*, vol. 2, no. 7, 2009.
- [6] J. Ikuno, M. Wulich, and M. Rupp, "System Level Simulation of LTE Networks," in *Proc. of the IEEE 71st Vehicular Technology Conference (VTC)*, Taipei, Taiwan, May 2010.
- [7] Y.-D. Yao and A. U. Sheikh, "Investigations into cochannel interference in microcellular mobile radio systems," *IEEE Transactions on Vehicular Technology*, vol. 41, no. 2, 1992.
- [8] C. A. Coelho, "The generalized integer gamma distributiona basis for distributions in multivariate statistics," *Journal of Multivariate Analysis*, vol. 64, no. 1, 1998.
- [9] A. Papoulis and S. U. Pillai, *Probability, Random Variables and Stochastic Processes*, 4th ed. McGraw-Hill Higher Education, 2002.
- [10] AWE-Communications. (2013, Aug.) Winprop. [Online]. Available: <http://www.awe-communications.com/>
- [11] Ericsson, Nokia, Motorola, and Rohde & Schwarz, "R4-070572: Proposal for LTE channel models," [www.3gpp.org](http://www.3gpp.org), 3GPP TSG RAN WG4, meeting 43, Kobe, Japan, May 2007.
- [12] E. Liu and K. K. Leung, "Fair resource allocation under rayleigh and/or rician fading environments," in *Proc. of IEEE 19th International Symposium on Personal, Indoor and Mobile Radio Communications, 2008.*, 2008, pp. 1–5.
- [13] D. Avidor, S. Mukherjee, J. Ling, and C. Papadias, "On some properties of the proportional fair scheduling policy," in *Proc. of 15th IEEE International Symposium on Personal, Indoor and Mobile Radio Communications, 2004.*, vol. 2, 2004.
- [14] O. Osterbo, "Scheduling and capacity estimation in LTE," in *Proc. of IEEE 23rd International Teletraffic Congress (ITC)*, 2011.
- [15] J.-M. Kelif, M. Coupechoux, and P. Godlewski, "On the dimensioning of cellular OFDMA networks," *Physical Communication*, vol. 5, no. 1, 2012.
- [16] T. Novlan, J. Andrews, I. Sohn, R. Ganti, and A. Ghosh, "Comparison of fractional frequency reuse approaches in the OFDMA cellular downlink," in *Proc. of 2010 IEEE Global Telecommunications Conference*, Dec. 2010, pp. 1–5.
- [17] T. D. Novlan, R. K. Ganti, A. Ghosh, and J. G. Andrews, "Analytical evaluation of fractional frequency reuse for heterogeneous cellular networks," *IEEE Transactions on Communications*, vol. 60, no. 7, 2012.



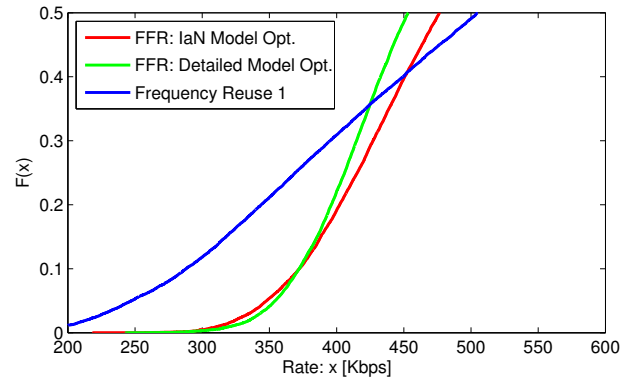
(a) FFR performance for 1 interferer (Site 3)



(b) FFR performance for 2 interferers (Site 3,4)



(c) FFR performance for 3 interferers (Site 3,4,7)



(d) FFR performance for 6 interferers.

Fig. 4: FFR performance for IaN and exact models